Acta Cryst. (1957). **10**, 53

Asymmetric Electron Diffraction Pattern from Molybdenite

By Ryozi Uyeda

Physical Institute, Nagoya University, Nagoya, Japan

and Shizuo Miyake

Tokyo Institute of Technology, Oh-Okayama, Meguro-ku, Tokyo, Japan

(*Received* 16 *July* 1956)

The electron diffraction pattern from the cleavage surface (0001) of molybdenite is asymmetric across the plane of incidence when the plane is parallel to the glide plane $(10\bar{1}0)$. By this asymmetry one can distinguish the sense of the polar axis of the first S–Mo–S layer on the boundary surface, i.e. one finds the polarity of a non-centrosymmetric layer in a centrosymmetric crystal. This is a more glaring contradiction to the results of the kinematical theory than the failure of Friedel's law because Friedel's law is concerned only with the polarity of a non-centrosymmetric crystal. An explanation of the phenomenon is given by the dynamical theory, and the relation between the phenomenon and failure of Friedel's law is discussed.

1. Introduction

Previously, Miyake & Uyeda (1950) reported an exception to Friedel's law in electron diffraction patterns from zincblende. Kohra, Uyeda & Miyake (1950) and Kohra (1954) explained this phenomenon by the dynamical theory of electron diffraction. Recently, Niehrs (1955) and Miyake & Uyeda (1955) examined the validity of Friedel's law in the dynamical theory from a more general point of view. They made it clear that Friedel's law does not always hold, even when no anomalous dispersion takes place.

In the present paper we report a new phenomenon which is found in the electron diffraction pattern from the cleavage surface of molybdenite. The phenomenon is remarkable because it enables us to distinguish the sense of the polar axes of the first S–Mo–S layer on the boundary surface, i.e. by the phenomenon we can distinguish the polarity of a non-centrosymmetric layer in a centrosymmetric crystal (Fig. 1). This is clearly a more glaring contradiction to the result of the kinematical theory than the failure of Friedel's law, because by the failure of Friedel's law only the polarity of a non-centrosymmetric crystal as a whole is distinguished. We explain the new phenomenon by the dynamical theory and discuss the relation between this phenomenon and the failure of Friedel's law.

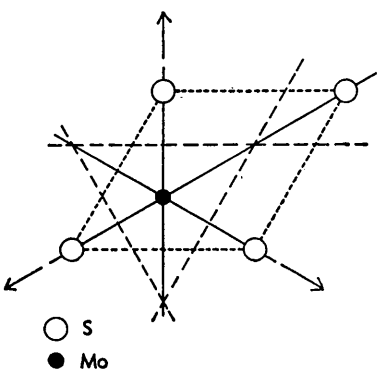

Fig. 1. The unit pattern of a S–Mo–S layer in molybdenite. Arrows: twofold polar axes of the layer. Solid lines: mirror planes of the crystal, parallel to $(11\bar{2}0)$. Broken lines: *c*-glide planes of the crystal, parallel to $(10\bar{1}0)$.

2. Experiment

We have studied electron diffraction patterns from the cleavage surface (0001) of molybdenite (MoS_2) by the reflexion method (Fig. 2). The space group of molybdenite is D^4_{6h}–$P6_3/mmc$ and the kinematical theory predicts patterns symmetric across the centre line, when the plane of incidence is parallel to the glide plane $(10\bar{1}0)$ or the mirror plane $(11\bar{2}0)$ (Fig. 1). Contrary to the prediction, we observed an asymmetric pattern in $(10\bar{1}0)$ (Fig. 3(*a*)), while we observed a symmetric pattern in $(11\bar{2}0)$ (Fig. 3(*c*)). To make clear the asymmetric feature of Fig. 3(*a*), it is illustrated in Fig. 3(*b*) somewhat exaggerated. The rotation photograph in $(10\bar{1}0)$ also shows asymmetry (Fig. 3(*d*)). Although the asymmetry is not so remarkable as to be

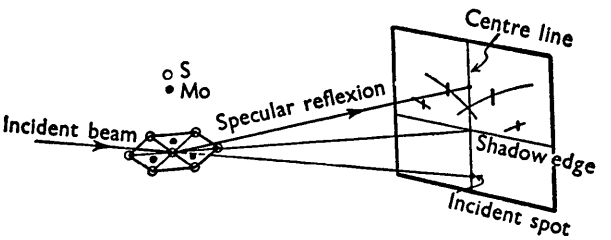

Fig. 2. Geometrical arrangement of the experiment. In this illustration the plane of incidence is $(10\bar{1}0)$ in which the asymmetry is observed.

(*a*)

(*c*)

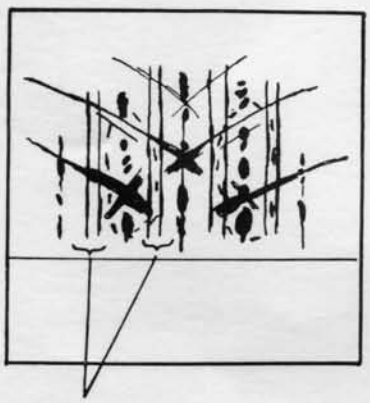

(*b*)

(*d*)

Fig. 3. Reflexion patterns from the cleavage surface of molybdenite.

(*a*) Asymmetric pattern in plane of incidence $(10\bar{1}0)$ (stationary crystal).
(*b*) Illustration of the asymmetry (compare the two parts indicated by broken lines).
(*c*) Symmetric pattern in plane of incidence $(11\bar{2}0)$ (stationary crystal).
(*d*) Asymmetric pattern in plane of incidence $(10\bar{1}0)$ (rotating crystal).

[*To face p.* 53

recognized at a glance, it cannot be overlooked. The asymmetry is not due to any mis-setting of azimuth, because the azimuth was most carefully adjusted in every case by observing the geometry of the Kikuchi pattern.

Previously, Kainuma & Uyeda (1950) found that an extra pattern is superposed on the molybdenite pattern, indicating an organic substance adsorbed on the cleavage surface of molybdenite. In the present experiment, too, the extra pattern was sometimes observed, as seen in Figs. 3(*c*) and 3(*d*).* However, it was confirmed that the asymmetry is not influenced at all by the superposition of the extra pattern, indicating that the asymmetry is caused by the molybdenite crystal itself.

The asymmetric pattern in $(10\bar{1}0)$ cannot be understood by a kinematical theory, because the absolute value of the structure amplitude of $(h0\bar{h}l)$ is equal to that of $(\bar{h}0hl)$. The asymmetry does not mean a failure of Friedel's law, because the molybdenite crystal has a center of symmetry. However, each single layer of S–Mo–S in molybdenite has no center of symmetry. It is trigonal, being symmetric across $(11\bar{2}0)$ but asymmetric across $(10\bar{1}0)$. We ascertained by experiment that the asymmetric pattern changes from, say, left-handed to right-handed by rotating the crystal through 60° about the *c* axis. Since this result is in accordance with the trigonal symmetry of the S–Mo–S layer, we believe that the observed asymmetry is directly related to the polarity of the layer on the boundary surface. Thus the sense of the polar axis of the uppermost layer of the crystal can be distinguished by observing the asymmetry.

Since two adjacent layers in the molybdenite structure have opposite polarities, the asymmetric pattern should change its sense when one S–Mo–S layer is peeled off the surface. Therefore, to observe the asymmetry, the cleavage surface used must be so perfect that it has no steps over the area irradiated by the incident beam. It has been shown previously by an experiment of oriented overgrowth of gold crystals that only good cleavage surfaces of molybdenite have no steps over a macroscopic area (Kainuma, 1951). If the samples used were not good enough, the asymmetry could not have been observed because of steps.

The detailed behavior of the asymmetry is somewhat complicated. This arises mainly from the complicated diffraction process itself, but in part it is due to the inevitable bending of the specimens; even for stationary crystals the bending causes diffraction patterns more or less resembling rotation photographs.

3. Interpretation by the dynamical theory

In this section the observed asymmetry is treated by the dynamical theory, without taking into account the effect of absorption. For the exact treatment of the phenomenon, we must take into account many diffracted waves which are coupled with one another. Since such a treatment is rather difficult, and since our observation is only qualitative, we treat here the problem qualitatively on the simplest assumption. This is sufficient for proving that the asymmetry does occur and that the sense of the asymmetry is reversed by peeling one layer of S–Mo–S off the surface.

Let us assume, according to the experimental condition, that the incident beam falls upon the cleavage surface of molybdenite at grazing incidence in the $(10\bar{1}0)$ plane (Fig. 2). The sphere of reflexion intersects on a circle the plane which contains reciprocal lattice points of the type $(h0\bar{h}l)$ (Fig. 4). Let us treat

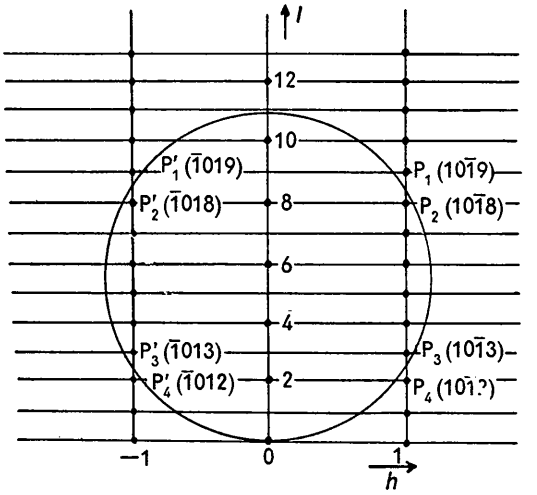

Fig. 4. Reciprocal lattice of molybdenite.

the case where eight lattice points $P_1(h0\bar{h}p)$, $P_2(h,0,\bar{h},p-1)$, $P_3(h0\bar{h}q)$, $P_4(h,0,\bar{h},q-1)$, $P'_1(\bar{h}0hp)$, $P'_2(\bar{h},0,h,p-1)$, $P'_3(\bar{h}0hq)$ and $P'_4(\bar{h},0,h,q-1)$ lie near the sphere. In Fig. 4 $h = 1$, $p = 9$ and $q = 3$.

We can calculate the amplitudes u_m of the diffracted waves inside the crystal by the fundamental equation of the dynamical theory (Bethe, 1928):

$$(\varkappa_0^2-\mathbf{k}_m^2)u_m+\sum_n{}'v_n u_{m-n} = 0\,, \qquad (1)$$

where*

$$\varkappa_0^2 = (2m/h^2)(E+eV_0),\quad v_n = (2me/h^2)V_n\,, \qquad (2)$$

$$\mathbf{k}_m = \mathbf{k}_0+\mathbf{h}_m\,. \qquad (3)$$

In (1) $\sum_n{}'$ is the sum over n except $n = (000)$. In (2) E is the kinetic energy of the incident electrons, V_0 the mean inner potential and V_n the nth Fourier coefficient of the crystal potential field. In (3) $\mathbf{k}_0$ is the wave vector of the primary wave inside the crystal and $\mathbf{h}_m$ the vector corresponding to the mth reciprocal-lattice point.

* The extra pattern disappears when the crystal is heated to about 150° C.

* The notation used in this section is the same as that used in our previous paper (Miyake & Uyeda, 1955).

We assume as an approximation that only the primary wave is strong, the eight diffracted waves weak, and all the other diffracted waves negligible. Then we can calculate the amplitudes of the eight waves by neglecting all the terms in the summation in (1) except $v_m u_0$. Thus the amplitudes become

$$u_s = -v_s/Q_s,\ u'_s = -v'_s/Q_s,\ (s = 1, 2, 3, 4)\,, \quad (4)$$

where s denotes the suffixes of the reciprocal-lattice points P_s or P'_s and the prime indicates the quantities relating to the points P'_s. The coefficient u_0 is normalized to unity and, according to the geometrical condition, Q_s is given by

$$Q_s = (\varkappa_0^2 - \mathbf{k}_s^2) = (\varkappa_0^2 - \mathbf{k}_s'^2)\,. \quad (5)$$

The wave field inside the crystal is represented by

$$u_c = \alpha \{\exp[2\pi i(\mathbf{k}_0.\mathbf{r})] + \sum_s{}' u_s \exp[2\pi i(\mathbf{k}_s.\mathbf{r})] + \sum_s u'_s \exp[2\pi i(\mathbf{k}'_s.\mathbf{r})]\}\,, \quad (6)$$

and the wave field outside the crystal by

$$u_U = A \exp[2\pi i(\mathbf{K}_0.\mathbf{r})] + R \exp[2\pi i(\mathbf{K}.\mathbf{r})] + R' \exp[2\pi i(\mathbf{K}'.\mathbf{r})]\,, \quad (7)$$

where $\mathbf{K}_0$ is the wave vector of the incident wave and $\mathbf{K}$ and $\mathbf{K}'$ are those of the diffracted waves. Since all the $\mathbf{k}_s$ have the same tangential component, only one diffracted wave with the wave vector $\mathbf{K}$ appears in a vacuum (Lamla, 1938; Laue, 1948). Similarly, also for $\mathbf{k}'_s$ only one diffracted wave with $\mathbf{K}'$ appears.

The amplitudes α, R and R' are determined by the conditions

$$u_c = u_U,\ \partial u_c/\partial z = \partial u_U/\partial z \quad (8)$$

on the boundary surface, where z is the coordinate normal to the surface. We first assume that the boundary surface passes through the origin of the coordinate. Then continuity of the wave function is expressed as

$$A = \alpha,\ R = \alpha \sum_s{}' u_s,\ R' = \alpha \sum_s u'_s\,, \quad (9)$$

and the continuity of the derivative as

$$A = \alpha(\gamma_0/\Gamma_0),\ R = \alpha(1/\Gamma)\sum_s{}' \gamma_s u_s,\ R' = \alpha(1/\Gamma')\sum_s \gamma'_s u'_s\,, \quad (10)$$

where γ_0, Γ_0, etc. are the normal components of $\mathbf{k}_0$, $\mathbf{K}_0$, etc. Thus we are given six equations for three unknowns. This paradox is due to our rough approximation, and we must follow some conventional way. For this purpose we take the mean of the corresponding equations in (9) and (10) and, for the sake of simplicity, we use approximate relations

$$\Gamma_0 = \gamma_0\,,$$
$$\Gamma = \Gamma' \approx \gamma_1 = \gamma'_1 \approx \gamma_2 = \gamma'_2 \approx -\gamma_3 = -\gamma'_3 \approx -\gamma_4 = -\gamma'_4\,. \quad (11)$$

Then R and R' follow as

$$R = A(u_1 + u_2),\quad R' = A(u'_1 + u'_2)\,. \quad (12)$$

In these equations the amplitudes u_3, u_4, u'_3 and u'_4 do not appear, only u_1, u_2, u'_1 and u'_2 appearing. This is justified physically because the amplitudes R and R', which are reflected from the crystal, are mainly determined by the amplitudes of waves which propagate outward in the crystal, and are little influenced by waves which propagate inward in the crystal.

To examine the relation between R and R' the relation between corresponding v's is required. Since $(10\bar{1}0)$ is a glide plane, we have a general relation

$$v_{h0\bar{l}} = (-1)^l v_{\bar{h}0l} \quad (13)$$

provided the origin lies on the glide plane. Therefore, we obtain by (4) the relation

$$u_1 = (-1)^p u'_1,\quad u_2 = (-1)^{p-1} u'_2\,, \quad (14)$$

where p is that p in the index $P_1(h0\bar{h}p)$. Substituting (14) into (12), we finally obtain

$$R = A(u_1 + u_2),\quad R' = \pm A(u_1 - u_2)\,, \quad (15)$$

where the two signs correspond to even and odd p. The absolute values $|R|$ and $|R'|$ are not equal, implying that the asymmetry appears for both even and odd p.

In deriving (15) we have assumed that the boundary surface passes the coordinate origin. If the boundary surface passes a distance d from the origin, (15) is replaced by

$$\left.\begin{aligned} R &= A\{u_1 + u_2 \exp[2\pi i(d/c)]\}\,, \\ R' &= \pm A\{u_1 - u_2 \exp[2\pi i(d/c)]\}\,. \end{aligned}\right\} \quad (16)$$

It should be noted that the phases of structure factors which influence the phases of u_1 and u_2 depend on the position of the coordinate origin. Let us first assume that the origin lies on a mid-plane between adjacent S–Mo–S layers. Then (15) represents the reflected amplitudes from a cleavage plane because a cleavage should occur on a mid-plane between the layers. Let us next assume that one S–Mo–S layer is peeled off the surface. Then, the reflected amplitudes are given by (16) with $d = \frac{1}{2}c$. Since in this case the phase factor in (16) is -1, we can conclude that R and R' in (15) are equal to R' and R, respectively, in (16). This implies that the asymmetry is reversed by peeling off one layer.

According to (15) or (16), the asymmetry occurs only when the amplitudes u_1 and u_2 of two adjacent Bragg reflexions are of the same order of magnitude. It vanishes when either amplitude vanishes. Therefore,

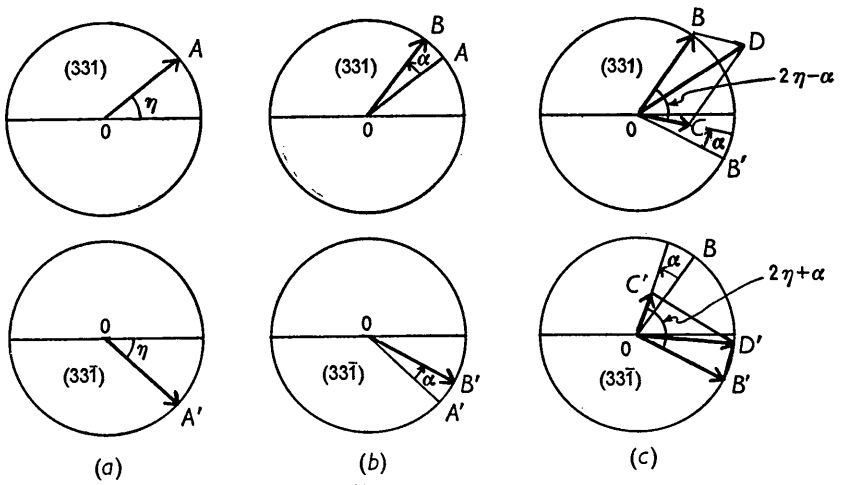

Fig. 5. Diagram illustrating amplitudes of (331) and (33$\bar{1}$) reflexions from zincblende (see explanation in the text). (*a*) Rea resonance defect, with no coupling. (*b*) Complex resonance defect, with no coupling. (*c*) Complex resonance defect, with coupling.

the asymmetry can be observed only when the intensity of reflexion does not vanish even at the middle of two adjacent Bragg reflexions. This condition is satisfied for molybdenite mainly by virtue of the large spacing of the cleavage plane. We can see on the rotation photograph (Fig. 3(*d*)) that, in fact, the reflexions are strong almost continuously between successive Bragg reflexions.

Concerning the validity of the above theoretical result, there may arise a doubt that the above treatment over-simplifies the actual situation to such an extent as to derive trivial conclusions. We can prove, however, that the same equation as (15) can be derived in a more exact treatment in which four reflexions corresponding to P_1, P_2, P_1', P_2' are assumed strong and all possible dynamical couplings among them are taken into account. However, we do not work out such a treatment here because the increased mathematical complication does not lead to any better physical understanding of the observed asymmetry.

4. Discussion

The explanation of the asymmetry observed for molybdenite gives a better understanding of the cause of the failure of Friedel's law for zincblende, because both phenomena are related intimately to each other. In this section the cause of the failure of Friedel's law is discussed, together with the cause of the occurrence of the molybdenite-type asymmetry.

Let us first consider the failure of Friedel's law for zincblende. According to Miyake & Uyeda (1950), the diffraction pattern is asymmetric when an incident wave falls upon the cleavage face (110) of zincblende in the plane of incidence (001); for example, the intensities of (331) and (33$\bar{1}$) are asymmetric. The physical meaning of the theoretical explanation of the phenomenon (Kohra *et al.*, 1950; Kohra, 1954; Miyake & Uyeda, 1955) can be summarized as follows:

The structure factors of (331) and (33$\bar{1}$) are complex conjugate to each other provided the origin of coordinates is chosen at the position of a zinc or sulphur atom. If there were no coupling between two reflexions, each amplitude would be given by the corresponding structure factor divided by the resonance defect.* When the resonance defect is real, the amplitudes of both reflexions are represented by vectors OA and OA' in the complex plane (Fig. 5(*a*)), η being the phase factor of (331). When, however, the resonance defect is complex, occurring in the range of total reflexion of the Bragg case, the amplitude is rotated away from the direction of the structure-factor vector through the phase angle α of the resonance defect. As the resonance defects of (331) and (33$\bar{1}$) are the same in the present case, the two amplitudes are rotated by α in the same sense, resulting in OB and OB' (Fig. 5(*b*)). Actually, however, there is coupling between (331) and (33$\bar{1}$), i.e. (331) is again reflected by (00$\bar{2}$), resulting in a new component OC' of (33$\bar{1}$), and similarly (33$\bar{1}$) is again reflected by (002), resulting in a new component OC of (331). The new components are also subjected to rotation through the phase angle α. It is thus evident that the final amplitudes OD and OD' of (331) and (33$\bar{1}$), given by the vector sums of the original and new components, are different in their absolute values (Fig. 5(*c*)). This implies that the diffraction pattern is asymmetric and Friedel's law fails.

From the above consideration we can say that the failure of Friedel's law is caused by *the interference between the new and the original components*. The interference occurs inside the crystal and we can say that

* See (4) of the present paper; for more exactness, see (29) of our previous paper (Miyake & Uyeda, 1955).

Friedel's law has already failed inside the crystal. Thus the asymmetry is independent of the position of the boundary surface (Kohra, 1954). Since, as will be referred to later, there are other causes for the failure of Friedel's law, we call the above cause the *first cause* of the failure. The failure due to this cause occurs under the two conditions that: (1) the coupling structure factors do not vanish, and (2) the reflexions are in the range of total reflexions.

Next, let us return to the molybdenite-type asymmetry. In this case the cause of the asymmetry is *the interference between two crystal waves which have the same tangential component.* The interference occurs outside the crystal when the crystal waves having the same tangential component are unified. Thus the feature of asymmetry depends on the position of the boundary surface. This asymmetry can occur even with a vanishing coupling structure factor and even outside the region of total reflexions. However, it cannot occur in the Laue case because the simultaneous excitation to considerable intensities is never possible for two diffracted waves having the same tangential component.

Miyake & Uyeda (1955, § 6) have pointed out that in addition to the first cause there is the *second cause* of the failure of Friedel's law. The second cause is also the result of the interference between crystal waves having the same tangential component. The interference process in this case is similar to that in the molybdenite-type asymmetry, but with the difference that in the former the wave vectors having the same tangential component belong to different wave points and are directed toward the same reciprocal-lattice point, while in the latter they belong to the same wave point and are directed toward different reciprocal-lattice points.

Finally, let us examine whether or not the molybdenite-type asymmetry can occur for non-centrosymmetric crystals. This is worth examining because, if the asymmetry can occur even only in principle, we have the *third cause* of failure of Friedel's law.

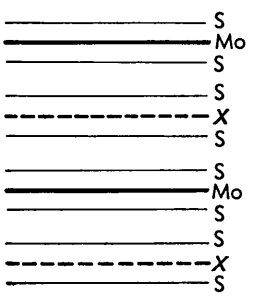

Fig. 6. Schematic illustration of the molybdenite-like model crystal.

For zincblende it can be proved that no asymmetry can occur provided the cleavage takes place on a midplane between two adjacent (110) atomic planes. In order to give an example in which the asymmetry occurs, let us consider, for example, a model crystal whose structure is molybdenite-like but in which all the molybdenum atoms on alternate layers are replaced by X atoms other than molybdenum (Fig. 6). This model crystal is evidently polar. For the Fourier coefficients of this structure we have the relation

$$v_{h0\bar{h}l} = (-1)^l v^*_{\bar{h}0hl}\,, \qquad (13')$$

corresponding to (13) for molybdenite. Therefore, under the same geometrical condition of the incident beam as for molybdenite (§ 3), we obtain, in place of (14), the relations

$$u_1 = (-1)^p u_1'^*, \quad u_2 = (-1)^{p-1} u_2'^*\,, \qquad (14')$$

and, in place of (15), the relations

$$R = A(u_1+u_2), \quad R' = \pm A(u_1^*-u_2^*); \qquad (15')$$

since $|R|$ is not equal to $|R'|$, the asymmetry occurs. Thus the molybdenite-type asymmetry can be the third cause of the failure of Friedel's law.

5. Conclusion

In electron diffraction, asymmetric patterns sometimes appear in violation of the rule of symmetry derived from the kinematical theory. The failure of Friedel's law, described in detail in the previous paper (Miyake & Uyeda, 1955), is a remarkable example of such violation. In the present paper another example of a more glaring violation is described and a theoretical explanation of it is given. It has been made clear that violations are essentially the effect of dynamical interference.

References

Bethe, H. (1928). *Ann. Phys., Lpz.* **89**, 55.
Kainuma, Y. (1951). *J. Phys. Soc., Japan*, **6**, 135.
Kainuma, Y. & Uyeda, R. (1950). *J. Phys. Soc., Japan* **5**, 199.
Kohra, K. (1954). *J. Phys. Soc., Japan*, **9**, 690.
Kohra, K., Uyeda, R. & Miyake, S. (1950). *Acta Cryst.* **3**, 479.
Lamla, E. (1938). *Ann. Phys., Lpz.* **32**, 178.
Laue, M. von (1948). *Materiewellen und ihre Interferenzen*, 2nd ed., chap. 5. Leipzig: Akademische Verlagsgesellschaft.
Miyake, S. & Uyeda, R. (1950). *Acta Cryst.* **3**, 314.
Miyake, S. & Uyeda, R. (1955). *Acta Cryst.* **8**, 335.
Niehrs, H. (1955). *Z. Phys.* **140**, 106.